Chapter 8

Gaussian Puff Modeling

Robert J. Yamartino

Integrals Unlimited, Portland, Maine (USA)
rjy@maine.rr.com

Abstract: This chapter focuses on the development of various Gaussian puff modeling techniques, with an emphasis on the relevant mathematics. Beginning with the diffusion equation, we first discuss the linkage between the 3D puff and plume formulations and show how the puff approach overcomes many of the limitations associated with plume modeling, including the limit of calm winds. The focus then shifts to consideration of the integral over source emission time and the integral-average over receptor time, both of which must be accomplished in an applied puff model. Puff model enhancements, including consideration of incorporating true puff dispersion coefficients and a detailed evaluation of the effect of wind shears on puff dispersion, conclude the chapter. No attempt has been made to duplicate discussions from Chapter 7B (e.g., summation of images, dry deposition) that are also directly applicable to puffs.

Key Words: Gaussian puff methods, atmospheric dispersion modeling.

1 Introduction

In both the preceding Chapter 7B and Chapter 7A from a previous volume (Vol. 1), the great simplicity and versatility of Gaussian plume formulations is evident. Extensive use of the plume formulation preceded that of the 3D puff because most near-field, high-impact source-receptor situations are adequately modeled by the plume and because the plume calculation can often be as computationally-simple as a "back-of-the-envelope" calculation; however, from a mathematical point of view, it is the puff which is more fundamental, deserving to be described first.

To rationalize exploring the more computationally-intensive puff modeling approach, one must recall the significant simplifications and approximations that were invoked to reach the Gaussian plume, including:

- the steady-state assumption, implying time-independent flow and turbulence fields as well as source conditions;
- neglect of most spatial gradients in flow and turbulence, though some shears can be approximated and plumes can be treated in a spatially-segmented fashion; and
- neglect of along-wind diffusion, though this can be shown to be related to the steady-state assumption.

How can one avoid these approximations and simulate transport and diffusion as accurately as possible, especially in low-wind or meandering wind situations? As mentioned above, "segmented-plume" models provide some relief, in that they can accommodate changing wind speed (i.e., for speeds over 1-2 m/s), wind direction, and stability class. However, even segmented-plume models ignore along-wind diffusion, and are thus inappropriate for extended calm periods.

Before delving into the puff in detail, consider first the most-detailed, opposite extreme to plume modeling. Perhaps, the ultimate method is to characterize pollutant emissions as consisting of many mathematical point particles, with each particle carrying information about:
- its current coordinates (x,y,z);
- the pollutant species mass(es) it represents; and,
- other possible "markers", such as its source name, emission time, and current density (i.e., for plume rise calculations).

Each particle can then be transported by the local flow (i.e., advective) and turbulent (diffusive) fields or conditions (e.g., statistical moments of turbulence) at each particle's current location. Of course, this approach is very close to mimicking the real emission process and is exactly the approach taken in Lagrangian particle modeling: many of the advantages of which are described in detail by Anfossi and Physick in Chapter 11 (Vol. 2). Unfortunately, this approach also has an important limitation arising from the fact that in order to compute a concentration, one must essentially "count" the particles at or near a receptor, and this process implies a level of statistical uncertainty. The process of computing concentrations can either be done by: (i) adding up the point particle masses within some finite-volume box imagined surrounding a receptor, and then dividing by the volume of the box; or, (ii) assigning each particle a sphere-of-influence, considering only those particles whose sphere-of-influence includes the specific receptor point, and adding the "partial concentration contributions" from each particle to yield a total concentration at the receptor. These "partial concentration contributions" are explicitly computed using a kernel estimator function, and there are many types of such kernel functions. For example, imagine that the mass of a particle is smeared uniformly over some sphere of radius R. Given that the 3D integral over this volume of $V = 4 \cdot \pi \cdot R^3 / 3$ must contain 100 % of the particle's mass, m, one is led to assign a concentration contribution of $C = m/V = 3 \cdot m/(4 \cdot \pi \cdot R^3)$ to receptors falling inside this radius of R and $C = 0$ to receptors outside of this radius. This kernel, K, of $1/V$ is seen to be

little different from the coupling coefficient of box- or plume-modeling, except that its units of m^{-3} is appropriate for a particle of discrete mass rather than the usual coupling coefficient units of s·m^{-3} associated with a source having a continuous mass emission rate expressed in g·s^{-1}.   This uniform density distribution kernel is not ideal, as it creates an unacceptable level of statistical noise due to its sharp drop in density at radius, R. What is preferred instead is a kernel that peaks at the location of the particle and falls off rapidly with distance. De Haan (1997) describes a variety of such kernel estimators and relates their properties (e.g., second moments) to that of the Gaussian kernel in one, two and three dimensions. In three dimensions the spherical kernel is given as:

$$K\left(x, y, z\right) = \frac{1}{(2\pi)^{3/2} \cdot \sigma^3} \cdot \exp\left[-\frac{r^2}{2\sigma^2}\right] \tag{1}$$

where $r^2 = (x - x_0)^2 + (y - y_0)^2 + (z - z_0)^2$ and the particle's current center is located at coordinates (x_0, y_0, z_0). Of course, this kernel is nothing more than a spherically symmetric Gaussian puff.

Thus, beginning with an emission of mathematical point particles, capable of precisely following the local flow and turbulence fields, coupled with the need to mitigate the statistical uncertainty noise associated with counting such particles, leads to a basic choice. One may either (1) increase the number of mathematical point particles emitted to a point where the statistical noise is acceptable, or (2) envision the particles as having their mass distributed over some volume in space. As the second choice is generally far less computationally intensive than the first, a rationale for puff modeling emerges. However, keep in mind that a weakness of this puff approach is that the larger the puff dimension, σ, the less the flow and turbulence sampling at the point (x_0, y_0, z_0) is representative of conditions over the entire puff. Thus, at the outset, one can realize the strength and weakness of the puff methodology in simulating air pollution problems.

In Chapter 7B, the 3D advection-diffusion equation (ADE) was given as:

$$\frac{\partial(\rho \cdot \phi)}{\partial t} = \underline{\nabla} \bullet [-(\underline{V} \cdot \rho \cdot \phi) + (\mathbf{K} \cdot \rho \cdot \underline{\nabla}\phi)] + (S - D) \tag{2a}$$

and

$$\frac{\partial C}{\partial t} = \underline{\nabla} \bullet [-(\underline{V} \cdot C) + (\mathbf{K} \cdot \rho \cdot \underline{\nabla}(C / \rho))] + (S - D) \tag{2b}$$

for the mixing ratio, φ, and mass concentration, C, respectively, and where scalar variables C, φ, ρ, S and D, vector wind field $\underline{V}$, and tensor (or 2D matrix) diffusivity $\mathbf{K}$ may generally all be 3D functions of x, y, and z. However, for the

simplified case of $\underline{V} = (u, v, w)$, with components u, v, and w and density ρ_0 uniform in space and time, and the rather sparse, diffusivity matrix of

$$\mathbf{K} = \begin{bmatrix} K_{xx} & 0 & 0 \\ 0 & K_{yy} & 0 \\ 0 & 0 & K_{zz} \end{bmatrix}, \text{ containing only the diagonal and space-time uniform,}$$

diffusivity elements, K_{xx}, K_{yy} and K_{zz} (or in their compressed notation form, K_x, K_y and K_z), one may write the solution of Eq.(2) as:

$$C(x,y,z,t) = \rho_0 \cdot \varphi(x,y,z) = m \cdot P(X,t) \cdot P(Y,t) \cdot P(Z,t) \qquad (3a)$$

where

$$X \equiv (x - x_0) - u \cdot (t - t_0), \quad P(X,t) = \frac{1}{\sqrt{2\pi}\sigma_x} \cdot \exp\left[-\frac{X^2}{2 \cdot \sigma_x^2} \right] \qquad (3b)$$

and where, for example,

$$\sigma_x^2 \equiv \sigma_{x0}^2 + 2 \cdot K_x \cdot (t - t_0). \qquad (3c)$$

Parallel expressions can be written for the corresponding Y and Z dependent variables, utilizing the velocity components v and w and the diffusivity components K_y and K_z, respectively. One also notes that the space-time zero point, (x_0, y_0, z_0, t_0), and initial dimension, σ_{x0}, may correspond to either the conditions at the time of initial release of mass m from the source or some other intermediate point in time (e.g., the conditions existing at the end of the previous computational time step in a multi-step model).

The similarity between Eq.(1) and Eq.(3) is no accident. As both equations are simply expressions of mass conservation and basically show that, under the stated uniformity conditions leading up to Eq.(3), the 3D Gaussian kernel, sometimes employed rather *ad hoc* in Lagrangian particle modeling, is identical to the solution of the 3D ADE for constant isotropic diffusivities.

Equation (3) is the core equation for all puff models and it will be used as the starting point for many calculations in the sections that follow. Also, it should be noted that much of what follows evolved during the development of the MESOPUFF II and CALPUFF models. Much of the material for these sections has been drawn from the "Model Formulation and User's Guide for CALPUFF" prepared by Scire et al. (1990b) for the California Air Resources Board.

The CALPUFF model has continued to evolve for nearly two decades, though many of the basic puff and integrated-puff equations described herein remain unchanged since the Scire et al. (1990b) document. The current version of

CALPUFF serves as a U.S. EPA Guideline model and is primarily documented in Scire et al. (2000).

2 Theoretical Background

2.1 The Puff-Plume Relationship

While the ability of Eq.(3) to be a solution of the 3D ADE is important, the fact that the normalization of the distribution functions over all space yields unity (i.e., 1.0) turns out to be more important from most practical considerations. For example, the space integral of $P(Z,t)$ over z yields:

$$N(Z, z_1, z_2) \equiv \int_{z_1}^{z_2} dz \cdot P(Z,t) = \frac{1}{2} \left[\begin{array}{c} erf[\dfrac{(z_2 - z_0) - u \cdot (t - t_0)}{\sqrt{2}\sigma_z}] - \\ erf[\dfrac{(z_1 - z_0) - u \cdot (t - t_0)}{\sqrt{2}\sigma_z}] \end{array} \right] \tag{4}$$

where

$Z \equiv (z - z_0) - u \cdot (t - t_0)$.

In the limit of integrating over all space (i.e., $z_1 \rightarrow -\infty$, $z_2 \rightarrow +\infty$), $N(Z, -\infty, +\infty) \rightarrow 1$, independent of the dependence of σ_z on time, t.

This same sort of integration also helps to bridge the transition between the puff and plume formulations. Rather than considering a few discrete puffs of mass m, imagine now a continuum of infinitesimal releases of size $Q \cdot dt'$, where continuous emission time t' takes the place of the discrete t_0. In order to achieve steady-state plume conditions, the source must have begun emitting long ago (e.g., at $t' = -\infty$) and still be emitting; whereas, the receptor might just have been turned on at time $t = 0$ and off at time $t = T$. Thus, to reach steady-state plume limit, one needs to consider Eq.(3) for the case where the vector wind aligns with the +x axis, so $\underline{V} = (u, 0, 0)$, and then compute the following double-time-integral of Eq.(3):

$$C(x,y,z) = \frac{Q}{T} \cdot \int_{-\infty}^{\infty} dt' \cdot \int_{0}^{T} dt \cdot P(X,t) \cdot P(Y,t) \cdot P(Z,t) \tag{5a}$$

where

$$X \equiv (x - x_0) - u \cdot (t - t') \tag{5b}$$

and the source is assumed to be located at $(x_0, y_0, z_0) = (0, 0, z_S)$.

While σ_y and σ_z may be some arbitrary function of puff age or transport time (i.e., $t\text{-}t'$), the plume material reaching the receptor will do so at a relatively constant transport time – an approximation that becomes more valid as the along-wind puff dimension, σ_x, is taken to be small relative to transport distance,
$x = u \cdot (t - t')$, that is:

$$\sigma_x \ll u \cdot (t - t') = x. \tag{5c}$$

Thus, we may rewrite $P(Y,t)$ and $P(Z,t)$ as:

$$P(Y,t) = \frac{1}{\sqrt{2\pi}\sigma_y} \cdot \exp\left[-\frac{y^2}{2 \cdot \sigma_y^{\,2}}\right] \text{ and } P(Z,t) = \frac{1}{\sqrt{2\pi}\sigma_z} \cdot \exp\left[-\frac{(z - z_S)^2}{2 \cdot \sigma_z^{\,2}}\right] \tag{5d}$$

and consequently, take these two terms outside the integrations of Eq.(5a).

This just leaves the $P(X,\ t\text{-}t')$ term inside the integrals. Now Eq.(5a) shows the emission time integration running from $t' = \text{-}\infty$ to $t' = \text{+}\infty$, even though it is obvious that any emissions later than $t' = T$ cannot possibly (i.e., via causality) contribute to the receptor concentration, but we choose the $t' = \text{+}\infty$ limit for simplicity. Note that Eq.(5a) actually indicates that one is <u>integrating</u> over emission time but <u>averaging</u> over receptor time, t. This is done because the time integral over receptor time yields an integrated-dose, whereas in Eq.(5a), one desires the average concentration, C. Now there are two ways to perform the double-integration. The more formal way involves integrating over receptor time, t, and the rotated variable $t'' \equiv t - t'$; however, as the actual plume concentration reaches steady-state, we note that the result of the receptor time integration must be $T/T = 1$, which reduces Eq.(5a) to a 1D integration, the result of which we already know from Eq.(4) to be:

$$C(x, y, z) = \frac{Q}{u} \cdot P(Y,t) \cdot P(Z,t). \tag{6}$$

This is just the Gaussian plume equation of Eq.(1) in Chapter 7B, with the exception that the wind velocity is explicitly given as the vector mean wind speed, u, rather than the more commonly used scalar wind speed, U. This is somewhat of a moot point for wind speeds in excess of 1 m/s, where the difference between the vector and scalar magnitudes is only a few percent. For very low wind speeds, the condition expressed by Eq.(5c) is no longer met, so the derivation of Eq.(6) would no longer be valid. Note that for very low wind speeds, the time dependence of the growth of the three σ quantities becomes important, such that the σ size values cannot be taken as "frozen" during the time of significant contribution of a puff to receptor's concentrations, and thus, cannot be subsequently ignored in the evaluation of Eq.(5a).

One can actually obtain a clearer understanding of what happens as $u \rightarrow 0$ by considering the case of a receptor at (0,0,0) and begin again with Eq.(5a). However, rather than assuming $\sigma_x << u \cdot (t - t')$, as in Eq.(5c), we will take the opposite limit of $\sigma_x >> u \cdot (t - t')$, and further assume that early plume growth proceeds as $\sigma_x = \sigma_u \cdot (t - t')$, with σ_y and σ_z showing corresponding dependencies on turbulent velocities σ_v and σ_w, respectively. In this case, Eq.(5a) becomes:

$$C(x,y,z) = \frac{Q \cdot \exp[-\frac{1}{2} \cdot (\frac{u}{\sigma_u})^2]}{(2 \cdot \pi)^{3/2} \cdot \sigma_u \cdot \sigma_v \cdot \sigma_w \cdot T} \cdot \int_0^T dt \cdot \int_\infty^0 dt'' \cdot \exp[-\frac{1}{2}(\frac{z_S}{\sigma_w \cdot t''})^2]/t''^3. \quad (7a)$$

The t'' integration yields $\Gamma(1)/t_0^2$ [1], where Γ is the Gamma function, with $\Gamma(1) = 1$, and the time-scale, t_0, is the diffusive transport time, $t_0 = z_S/\sigma_w$. Combining this result with the factor T coming from the receptor time integration, Eq.(7a) finally yields:

$$C(x,y,z) = \frac{Q \cdot \exp[-\frac{1}{2} \cdot (\frac{u}{\sigma_u})^2]}{[(2 \cdot \pi)^{1/2} \cdot \sigma_u] \cdot [(2 \cdot \pi)^{1/2} \cdot \sigma_v \cdot t_0] \cdot [(2 \cdot \pi)^{1/2} \cdot \sigma_w \cdot t_0]}. \quad (7b)$$

This result is very similar to the concentration estimated from Eq.(6), with the σ_y and σ_z values given as shown, except that the vector mean wind has been replaced by the quantity $(2 \cdot \pi)^{1/2} \cdot \sigma_u$. This factor of $(2 \cdot \pi)^{1/2}$ is somewhat unexpected, as the scalar wind speed, U, is generally given as $U = (u^2 + \sigma_u^2)^{1/2}$, but one must remember that as $u \rightarrow 0$, the diffusion occurs in both the "upwind" and "downwind" directions (i.e., if such directions can still be thought to exist at $u = 0$). In fact, this factor $(2 \cdot \pi)^{1/2}$ is exactly the conversion factor from Gaussian to the "box" normalization we have seen in Chapter 7B. That is, while advection will sweep out a dilutionary box of length $u \cdot \Delta t$ in a time Δt, the effect of a diffusive turbulent velocity will lead to a box length of $(2 \cdot \pi)^{1/2} \cdot \sigma_u \cdot \Delta t$. Hence, if one were to piece together an effective "dilutionary velocity" for the Gaussian plume model, it would not be U (i.e., what is commonly defined as the scalar wind speed), but rather the new velocity variable, $U' \equiv (u^2 + 2 \cdot \pi \cdot \sigma_u^2)^{1/2}$. Again, for moderate wind speeds, this second term is only a few percent of the contribution by u^2. Equation (7b) was obtained without invoking the need for the "frozen σ" approximation; however, given the widespread applicability of this approximation for even low wind speeds, we will have occassion to revisit it often in this chapter.

2.2   Practicality Constraints for Puff Models

Now that we understand the theoretical linkage between the puff and plume model, the connection between puff and Lagrangian particle models, and some of

---

[1] $\int dt \cdot \exp(-a \cdot t^p)/t^q = a^{(1-q)/p} \cdot \Gamma((1-q)/p, a \cdot t^p) / p$ from http://integrals.wolfram.com , where $\Gamma(\alpha, x)$ is incomplete Gamma function. Definite integral from Prudnikov et al., Vol. 1, pg 345, #2.3.18.2.

the advantages and limitations of puff models relative to the modeling techniques at the simpler (i.e., the Gaussian plume) and more computationally intensive (i.e., particle modeling) ends of the modeling spectrum, we have to decide what we really expect a practical puff model to deliver. The feature wish list can indeed grow quite long, but to become a useful regulatory model, a viable puff model must:

- deliver predictions that closely match plume predictions when conditions appropriate to the plume formulation pertain (e.g., steady-state emissions and dispersion conditions);
- avoid pitfalls associated with requiring data that is rarely available (e.g., accurate fields of vertical velocities, w)
- allow at least as much flexibility as plume models to include a variety of source types (e.g., points, areas, lines, volumes), near-source dynamical effects (e.g., plume rise, building wake effects), and loss mechanisms (e.g., dry/wet deposition, exponential decay); and,
- permit realistic scenarios (e.g., involving hundreds of sources, thousands of receptors, on a domain a large as a few thousand kilometers) to be performed for time periods as long as five years using present-day and widely-available computers.

Though the latter of these constraints is clearly not static, as computers become faster and cheaper, other constraints, such as providing accurate 3D winds (including w), are also evolving over time. Thus, the design of a practical model must be flexible enough to facilitate evolution of the model's capabilities.

Much of the history of puff model development has been driven by the first of the above constraints, that is, to deliver predictions that closely match plume predictions when conditions appropriate to the plume formulation pertain. However, it is not immediately obvious that a finite series of discrete puffs will yield the continuous plume result. Early puff models (e.g., Ludwig et al., 1977; van Egmond and Kesseboom, 1983; Peterson, 1986) evaluated the contribution of a puff to the concentration at a receptor by a "snapshot" approach. Each puff was considered "frozen" at particular time intervals or sampling steps, and the concentration due to the "frozen" puff at that time was computed or sampled. The puff was then allowed to move and evolve in size and mass until the next sampling step. The total concentration at a receptor was then just the <u>sum</u> of the contributions of all nearby puffs <u>averaged</u> over all sampling steps within the basic time step. Depending on the model and the application, the sampling and averaging time steps could be one hour (or longer), indicating that only one "snapshot" of the puff is utilized each hour. In this case, a problem immediately arises because there will be holes (or gaps) in the plume concentration precisely where there are spaces between the discrete puffs.

Thus, a traditional drawback of the puff approach has been the need for the release of many puffs to adequately represent a continuous plume close to a source. Ludwig et al. (1977) have shown that if the distance between puffs

exceeds about $2 \cdot \Phi_y$, inaccurate results may be obtained. Figure 1 shows that reasonable results are obtained for puff separations of no more than Φ_y. If the puffs do not overlap sufficiently, the concentrations at receptors located in the gap between puffs at the time of the "snapshot" are underestimated. While the normalization used in Figure 1 fixes the concentration at unity at the puff center, an un-normalized plot would show that for puff separations exceeding Φ_y, concentrations near the puff centers are overestimated. Ludwig et al. (1977) recommended spacing puffs uniformly in space, rather than in time, with a puff merging/purging scheme to reduce the total number of puffs.

As visualized in Figure 2, Zannetti (1981) suggested tracking fewer puffs than necessary for adequate sampling, but then saturating the area near a receptor with synthesized, interpolative puffs, in order to provide the required puff overlap.

Although both schemes act to reduce the number of puffs carried by the model, considering puffs as "snapshots" in space and time still requires that an uneconomically large number of puffs be generated near the source. For example, at a receptor 100 meters from a source, and assuming Pasquill-Gifford-Turner (PGT) dispersion rates, puffs at a density corresponding to a release rate of over 1300 puffs/hour are required to meet the two-Φ_y criterion for F stability, 3 m/s wind conditions. During high wind speed, neutral conditions (10 m/s, D stability), nearly 2200 puffs/hour are needed. The more stringent, one Φ_y criterion, would double the number of puffs required.
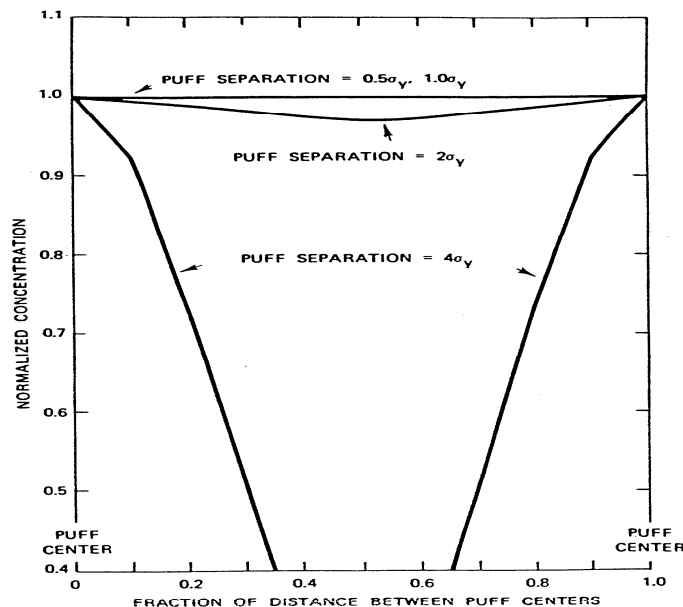
Figure 1. Normalized concentration between two puffs within a series of puffs having equal size and spacing. [From Ludwig et al., 1977.]
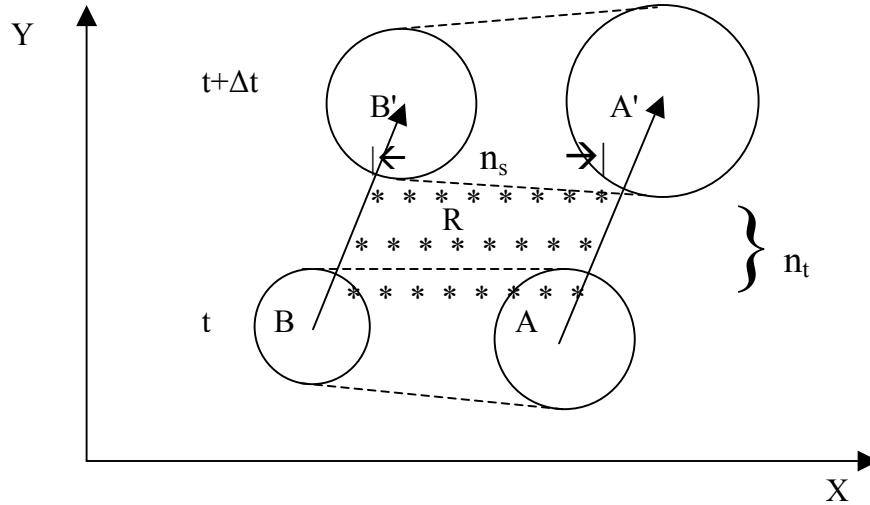
Figure 2. Illustration of the puff generation scheme of Zannetti (1981). A plume is represented by puffs A and B at time t. Subsequent transport moves these puff centers to locations A' and B' at time t+Δt. Concentrations at receptor R will not be well approximated by these four puffs, so they are subdivided into nₛ puffs in space at nₜ sub-time intervals. Such interpolative puffs are shown by the ₓ symbol. [From Zannetti, 1981.]

2.3   Integral Approximations for Sampling and Continuous Emissions

Faced with the high computational cost of sampling so many puffs, something had to be done to simplify the problem for a majority of cases, including:

- the far field where many large size puffs contribute to each receptor; and,
- the near field of continuous point sources where many hundreds of puffs and sampling sub-time-steps might be needed to emulate a continuous point source to avoid incurring holes in the concentration field.

Where approximations must be made can be better seen by considering the snapshot concentration contribution from a puff to a receptor located at space-time coordinates, (x, y, z, t). This instantaneous level can be simply written as:

$$C(x,y,z,t) = Q \cdot P(d_a, \sigma_a) \cdot P(d_c, \sigma_c) \cdot P_z \qquad (8a)$$

where

$$P(d_\beta, \sigma_\beta) \equiv P(d_\beta, \sigma_\beta, t) \equiv \frac{1}{\sqrt{2\pi} \cdot \sigma_\beta} \cdot \exp\left[-\frac{d_\beta^2}{2 \cdot \sigma_\beta^2}\right] \qquad (8b)$$

with subscript β denoting alongwind and crosswind axis subscripts a and c, respectively, such that d_a and d_c are the respective alongwind and crosswind distances from the puff center to the receptor, and where

$$P_z \equiv [P(z - z_S, h, \sigma_z, t) + P(z + z_S, h, \sigma_z, t)] \tag{8c}$$

with

$$P(z \pm z_S, h, \sigma_z, t) = \frac{1}{\sqrt{2\pi} \cdot \sigma_z} \cdot \sum_{j=-\infty}^{j=+\infty} \exp\left[-\frac{(z \pm z_S + 2jh)^2}{2 \cdot \sigma_z^2} \right]. \tag{8d}$$

Note that this is a slightly different use of the notation for the function P from previous use, in that the plume standard deviations are now explicitly referenced and explicit inclusion of the time variable has been suppressed. The time variable has been explicitly dropped as nearly every variable in Eq.(8), including Q, d_a, d_c, z_S, σ_a, σ_c, and σ_z, can be an explicit or implicit functions of time; thus, rendering explicit display of the time variable rather academic.

As in the case of Gaussian plume modeling (Chapter 7B), z_S is the effective source height of the puff above the ground and h is the mixed-layer depth. Similarly, the vertical term, P_z, includes the multiple reflections from the ground and inversion lid, and rapidly converges to the uniformly mixed limit of $P_z = h^{-1}$ for $\Phi_z > 1.6 \, h$. In general, puffs within the convective boundary layer meet this criterion within a few hours after release, permitting some level of simplification for models designed solely for mesoscale through long-range transport.

Nevertheless, having so many of the variables present in Eq.(8) being time-dependent suggests that performing integral summing over emission time and integral averaging over receptor time may be a formidable task. Two alternatives to the conventional snapshot sampling function are discussed below. Both utilize the previously-discussed "frozen Φ" approximation to avoid having time-dependence in the denominators of the exponential terms (i.e., due to time-dependent dispersion, Φs), though the rationales used for invoking this approximation differ.

2.3.1   The MESOPUFF Integrated Puff Sampling Formulation

The MESOPUFF II model (Scire et al., 1984a, b) introduced the notion of an integrated puff sampling function and also provided some simplifications for near-field applications. In the far-field, the developers assumed that over a given time step, puffs in the far-field grow fractionally by only a small amount such that frozen dispersion Φs might be presumed. They further assumed that these receptor-specific, frozen sigmas could be obtained by interpolating between the puff sigmas at the beginning and end of the time step to the downwind distance associated with the point of closest approach. In the cases where the downwind point of closest approach was beyond the beginning- or end-point of the puff trajectory segment, the nearest end-point sigma values were utilized. In addition, this integrated puff sampling scheme assumed radially-symmetric Gaussian puffs.

For a horizontally symmetric puff with $\Phi \equiv \Phi_a = \Phi_c$, Eq.(8a) reduces to:

$$C(x,y,z) = Q \cdot P(R,\sigma) \cdot P_z \qquad (9a)$$

where

$$P(R,\sigma) \equiv P(d_a,\sigma_a) \cdot P(d_c,\sigma_c) = \frac{1}{2 \cdot \pi \cdot \sigma^2} \cdot \exp\left[-\frac{R^2}{2 \cdot \sigma^2}\right] \qquad (9b)$$

where R is the receptor to puff center distance, such that, $R^2 = d_a^2 + d_c^2$. Now consider the parametric variable, p, conceived so that $p = 0$ at the beginning of the time step and $p = 1.0$ at the end of the time step. Consider a puff moving from initial coordinates (x_1, y_1) at $p = 0$ to final coordinates (x_2, y_2) for $p = 1$. Assuming the puff trajectory segment is a straight line, the radial distance to a receptor at (x,y) in terms of the parameter p is: $R^2 = (x_1 + p \cdot dx - x)^2 + (y_1 + p \cdot dy - y)^2$, where $dx \equiv x_2 - x_1$ and $dy \equiv y_2 - y_1$. Furthermore, one may assume that any changes in the puff's mass due to wet and dry removal processes can also be linearized such that, $Q(p) = Q(0) + p \cdot \Delta Q$, with $\Delta Q \equiv Q(1) - Q(0)$ typically being negative for loss mechanisms. Finally, freezing the value of the sigmas to their midpoint values at $p_m = 0.5$, such that $\Phi \equiv \Phi(p_m)$ and $\Phi_z \equiv \Phi_z(p_m)$, enables one to express the time-averaged receptor concentration over the time period T as:

$$\overline{C} \equiv \frac{1}{T} \int_t^{t+T} dt \cdot C(x,y,z,t) = \frac{P_z}{2 \cdot \pi \cdot \sigma^2} \cdot \int_0^1 dp \cdot Q(p) \cdot P[R(p),\sigma] \qquad (10)$$

where P_z has been taken outside the integration for the most typical case, the puff centerline height does not change over the time averaging period, and the sole dependences on p remain in the puff mass Q and the radial distance function, R. Re-expressing R^2/σ^2 as $a \cdot p^2 + 2 \cdot b \cdot p + c$ within the exponential, with a, b and c given as:

$a = (dx^2 + dy^2)/\sigma^2$,

$b = [dx \cdot (x_1 - x) + dy \cdot (y_1 - y)]/\sigma^2$, and

$c = [(x_1 - x)^2 + (y_1 - y)^2]/\sigma^2$.

"Completing the square" (see Chap 7B) within the integrand, one is left with integrands of the form $\exp(-x^2)$ and $x \cdot \exp(-x^2)$, that are known integrals, so the results may be expressed as:

$$\overline{C} = \frac{P_z}{2 \cdot \pi \cdot \sigma^2} \cdot [Q(0) \cdot I_1 + \Delta Q \cdot I_2] \qquad (11a)$$

where

$$I_1 = \left[\frac{\pi}{2a}\right]^{1/2} \exp\left[\frac{b^2}{2a} - \frac{c}{2}\right]\left\{erf\left[\frac{a+b}{(2a)^{1/2}}\right] - erf\left[\frac{b}{(2a)^{1/2}}\right]\right\}$$

and   (11b)

$$I_2 = \frac{-bI_1}{a} + \frac{1}{a}\exp\left[\frac{b^2}{2a} - \frac{c}{2}\right]\left\{\exp\left[\frac{-b^2}{2a}\right] - \exp\left[\frac{-1}{2}\left(a + 2b + \frac{b^2}{a}\right)\right]\right\} .$$

As mentioned, both the horizontal dispersion coefficient, Φ, and the vertical term, P_z, are evaluated and held constant throughout the trajectory segment and are computed at the mid-point (i.e., $p = 0.5$) of the segment in MESOPUFF II.

Again, at mesoscale distances, the fractional change in the puff size during the sampling step is usually small, and the use of the mid-point values of Φ and P_z is adequate. This assumption also reduces the number of times that the dispersion coefficients and vertical reflection terms need to be computed to once per sampling step (independent of the number of receptors). However, this optimization for mesoscale distances may not be appropriate in the near-field where the fractional puff growth rate can be rapid and plume height may vary. For this reason, the integrated sampling function for the CALPUFF model (Scire et al., 1990b) was implemented with receptor-specific values of Φ and P_z, evaluated at the point of closest approach of the puff to each receptor. This point was initially limited to the $p = 0$ thru $p = 1.0$ physical segment of the puff's trajectory, although some extension beyond these end-points by a fractional amount of the end-point sigma values was implemented in the code to ensure self-consistent results.

2.3.2   The CALPUFF Slug Formulation and Sampling Functions

The integrated puff sampling function approach ensures that puffs are properly sampled by the receptor, but this does not ensure that the puffs are spaced closely enough to ensure proper representation of a continously emitted plume. To accomplish this, one must either emit puffs at a rapid enough rate (i.e., the dilemma faced in earlier puff models) or develop a methodology to account for both continuous emission and integral-average receptor sampling. This latter methodology can be achieved only if one is able to perform the double-integral over both emission time, t', and receptor time, t. This same double-integral was considered in Eq.(5) with the accompanying discussion showing the linkage between the puff and plume formulations; however, the same integrals are not considered using a finite emission duration beginning at time $t' = 0$ and ending at $t' = t_E$, with the understanding that the $t_E \leq t$, the current sampling time, and the latest time which causality tells us can contribute to any impact. For the case of a source located at (x_0, y_0, z_0) and wind aligned with the x-axis, the receptor concentration, $C(x,y,z,t)$, integrated over emission time, t', is now:

$$C(x,y,z,t) = Q \cdot P(Y,\sigma_y) \cdot P(Z,\sigma_z) \cdot \int_0^{t_E} dt' \cdot P(X,\sigma_x, t-t') \qquad (12)$$

where $X \equiv (x - x_0) - u \cdot (t - t')$, $Y = y - y_0$, and $Z = z - z_0$.

Note that the $P(Y,\sigma_y)$ and $P(Z,\sigma_z)$ functions have already been taken outside the integral. In the discussion accompanying Eq.(5), this was justified on the basis of assuming the condition of Eq.(5c), that is, that along-wind diffusion was much smaller than the relevant transport distance to the receptor, or $\sigma_x << x$. Shrinking σ_x has the effect of forcing all the impact of emissions at time t' to be experienced at the receptor at the fixed time difference, $t - t' = x/u$, which in turn forces the dispersion coefficients, $\sigma(t - t')$, to take on fixed (or "frozen"), receptor-specific values. In the more general case of larger σ_x, where a wider range of time differences (i.e., $t - t'$), and hence differing σ values, contribute to the concentration, we continue to apply the "frozen σ" approximation, on the practical grounds that it links one back to the Gaussian plume formulation for which the empirical σ functions were determined from experiment in the first place. This insistence on a firm linkage to the Gaussian plume formulation is also a constraint imposed by regulatory agencies, which would be hard-pressed to explain why their puff model, run under conditions that emulate steady-state conditions, did not give the same answer as their plume model.

Performing the t' integration in Eq.(12) then yields the result:

$$C(x,y,z,t) = Q \cdot P(Y,\sigma_y) \cdot P(Z,\sigma_z) \cdot (F/u) \qquad (13a)$$

where F is the causality factor given as:

$$F = \frac{1}{2} \cdot \left\{ erf\left[\frac{x - u \cdot (t - t_E)}{\sqrt{2}\sigma_x(t - t_E)} \right] - erf\left[\frac{x - u \cdot t}{\sqrt{2}\sigma_x(t)} \right] \right\}. \qquad (13b)$$

Consistent with the discussion in Section 2.1, considering the limit of the vector mean wind, $u \rightarrow 0$, and to ensure a better match with the Gaussian plume, the factor $1/u$ is shifted to $1/U$ in terms of the scalar wind, and a factor, u/U is injected into the crosswind component to ensure that the sense of "crosswind" versus "downwind" vanish at $u = 0$.

The final expression for the snapshot concentration field due to such a pollutant "slug" then can be written as:

$$C(x,y,z,t) = Q \cdot P'(Y,\sigma_y) \cdot P(Z,\sigma_z) \cdot (F/U) \qquad (14a)$$

where

$$P'(Y, \sigma_y) \equiv \frac{1}{\sqrt{2\pi}\sigma_y} \cdot \exp\left[-\frac{d_c^2}{2 \cdot \sigma_y^2} \cdot \frac{u^2}{U^2} \right] \qquad (14b)$$

the causality factor F is re-expressed as:

$$F = \frac{1}{2} \cdot \left\{ erf\left[\frac{d_{a2}}{\sqrt{2}\sigma_{y2}} \right] - erf\left[\frac{-d_{a1}}{\sqrt{2}\sigma_{y1}} \right] \right\} . \qquad (14c)$$

This form now matches the formulation used in the CALPUFF model (Scire et al., 1995). Note that to achieve this match, the additional assumption, $\sigma_x = \sigma_y$, was injected for simplicity, and the distances d_c and d_a introduced as the cross-slug (i.e., perpendicular to the slug axis) and along-slug distances, respectively, to the receptor. In particular, d_{a2} is the receptor distance from the "youngest" slug end 2 (with $d_{a2} > 0$ in the direction of end 1), that is $d_{a2} = x_R - x_2$, whereas the receptor distance from the "oldest" slug end 1 is defined as:

$$-d_{a1} = d_{a2} - \ell_{xy,} = x_R - x_2 - (x_1 - x_2) = x_R - x_1 \qquad (14d)$$

where ℓ_{xy} is the length of the slug projection in the x-y plane, and where $\ell_{xy} = u \cdot t_E$ in this case. Again, the subscripts 1 and 2 on the dispersion coefficients refer to values at the "oldest" and "youngest" ends of the slug, respectively, while the absence of a numerical subscript indicates a value defined at the receptor.

This "slug" formulation retains many of the important properties of the circular puff model, while significantly reducing puff overlap problems associated with snapshot sampling of circular puffs. As it must, Eq.(14) explicitly conserves mass. As with circular puffs, each slug is free to evolve independently in response to the local effects of dispersion, chemical transformation, removal, etc. Also, the concentration distribution within the body of the slug, well away from the slug endpoints, approaches that of the Gaussian plume distribution. Finally, the concentrations near the endpoints of the slug (both inside and outside of the body of the slug) fall off in such a way that if adjacent slugs are present, the plume predictions will be reproduced when the contributions of those slugs are included (again, during steady-state conditions). This property can be proven by imagining that the previously emitted slug has ends labeled 0 and 1, with the #0 end being the oldest, and the newest end #1, coincident with the current #1 end representing the oldest part of the current release (i.e., the new end point of a previously released slug is co-located with the old end point of the slug subsequently released). This means that the summed concentration distribution from the two slugs will be:

$$C(x,y,z,t) = \frac{Q}{U} \cdot P'(Y,\sigma_y) \cdot P(Z,\sigma_z) \cdot \frac{1}{2} \cdot \left\{ \begin{array}{l} erf\left[\dfrac{x_R - x_2}{\sqrt{2}\sigma_{y2}}\right] - erf\left[\dfrac{x_R - x_1}{\sqrt{2}\sigma_{y1}}\right] + \\[2mm] erf\left[\dfrac{x_R - x_1}{\sqrt{2}\sigma_{y1}}\right] - erf\left[\dfrac{x_R - x_0}{\sqrt{2}\sigma_{y0}}\right] \end{array} \right\}$$

or, with cancellations, this becomes:

$$C(x,y,z,t) = \frac{Q}{U} \cdot P'(Y,\sigma_y) \cdot P(Z,\sigma_z) \cdot \frac{1}{2} \cdot \left\{ erf\left[\frac{x_R - x_2}{\sqrt{2}\sigma_{y2}}\right] - erf\left[\frac{x_R - x_0}{\sqrt{2}\sigma_{y0}}\right] \right\}. \quad (15)$$

Thus, assuming meteorology and emissions remain unchanged, consecutively released slugs combine to form a longer single slug, and ultimately, if the process is repeated, would form a complete Gaussian plume.

This fact illustrates the concept that the "causality" function, F, accounts for edge effects near the endpoints of the slug. For long emission times, such that $u \cdot t_E \gg \Phi_x$, and points well inside the body of the slug, evaluation of the error functions in Eq.(14c) produces: $F = 0.5 \cdot (1 - (-1)) = 1$ (i.e., no edge effects). For receptors well outside the slug, F becomes zero, indicating that the pollutant material has not yet reached the receptor or has already passed it. Near the endpoints, the causality factor produces a leading/trailing Gaussian-like tail on the distribution.

The factor (u/U) allows low wind speed and calm conditions to be properly treated. As u approaches zero, the exponential crosswind term becomes unity and $F \rightarrow -erf[d_a / (\sqrt{2}\sigma_y)]$. Under these conditions, the radial concentration dependence of the distribution is determined by the causality factor. For u greater than a few meters per second, (u/U) is very close to one, so that this ratio becomes unimportant. The factors (u/U) and F make the slug model more "puff-like" than segmented plume models (e.g., Hales et al., 1977; Benkley and Bass, 1979). Also, unlike the slug model, segmented plume models generally do not properly treat low wind speed conditions or segment edge effects.

Equation (14) represents a "snapshot" description of the elongated puff or slug at time t; however, as with the "snapshot" puff equation, Eq.(14) must be integrally-averaged over the receptor's sampling time step to produce a time-averaged concentration, $\overline{C}(x,y,z)$. In the case where the emission rate and meteorological conditions do not vary during the sampling step, a generalized analytical solution to the integral can be obtained for "emitted" slugs (i.e., where the endpoint of the "youngest" end of the slug is at the source) as:

$$\overline{C}(x,y,z) = \frac{Q}{U} \cdot P'(Y,\sigma_y) \cdot P(Z,\sigma_z) \cdot \overline{F} \qquad (16a)$$

where the time-averaged causality factor, $\overline{F}$, is given as:

$$\overline{F}=\frac{1}{2}\cdot erf(\phi_2)+\frac{1}{2}\cdot\frac{\sqrt{2\cdot\sigma_y}}{u\cdot\Delta t_S}\cdot\left\{[\xi_e\cdot erf(\xi_e)-\xi_b\cdot erf(\xi_b)]+\frac{1}{2}\cdot\left[\exp(\xi_e^2)-\exp(\xi_b^2)\right]\right\}\ (16b)$$

and where,

> $\xi_b\equiv d_{a2}/(\sqrt{2}\sigma_y)$ accounts for the <u>beginning</u> of the sampling time step,
>
> $\xi_e\equiv(d_{a2}-u\cdot\Delta t_S)/(\sqrt{2}\sigma_y)$ represents the <u>end</u> of the sampling step, and
>
> $\phi_2\equiv d_{a2}/(\sqrt{2}\sigma_{y2})$ represents the steady-state conditions at the source, with
>
> Φ_{y2} representing any initial lateral spread of the emissions at the source.

Note that Eq.(16) applies to the case where the sampling interval, $(0, \Delta t_S)$, is the same as the emission interval, $(0, t_E)$, as is normally the case for fresh, continuous emissions (i.e., since emissions for $t_E > \Delta t_S$ cannot causally contribute). However, as the indefinite integral, $\int dx\cdot erf(x)=x\cdot erf(x)+\exp(-x^2)/\sqrt{\pi}$ exists, the more general solution could have been written.

For older slugs, the endpoint of the slug is no longer fixed at the source and the long axis of the slug is not necessarily along the current advecting wind direction. Additionally, the two end points may experience different winds, causing rotation and stretching of the slug. In this general case, an analytical integration of Eq.(14) is not possible for such slugs unless restrictive conditions are imposed on the form of the puff growth equations. Because of the importance of generality in the puff growth equations, the time-averaged concentrations associated with older slugs are determined via numerical integration of Eq.(14) and such integration can generally be accomplished at reasonable computational cost. For example, Figure 3 displays the snapshot concentration isopleths of a slug at the beginning (left) and end (right) of a particular sampling time step, whereas Figure 4 shows the result of the numerical integral averaging over the same time interval.

The above development also ignores the effect of loss or production mechanisms; however, this can be handled in much the same "linearized" manner that MESOPUFF II invokes. This is accomplished by allowing the effective emission rate, Q, to vary linearly over time as:

$$Q(t) = Q_b + (Q_e - Q_b)\cdot(t/\Delta t_S) \qquad (17)$$

where Q_b is the effective emission rate for the slug at the beginning of the time step (note that $Q_b = Q$ for fresh emissions), Q_e is the effective emission rate including loss or production which occurs during the time step, and Δt_S is the duration of the time step.
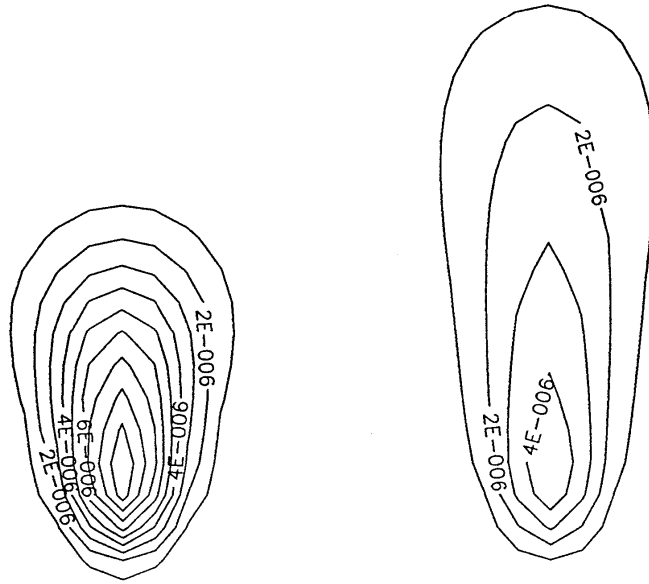
Figure 3. Isopleths of a slug "snapshot" at two points in time. The slug at left shows concentrations at some early time, whereas the snapshot at right shows the isopleths of the same slug at a later time. During the intervening time, the slug clearly experienced advection (to the right), diffusion, and some along-slug stretching due to wind shear. [From Scire et al., 1990b]
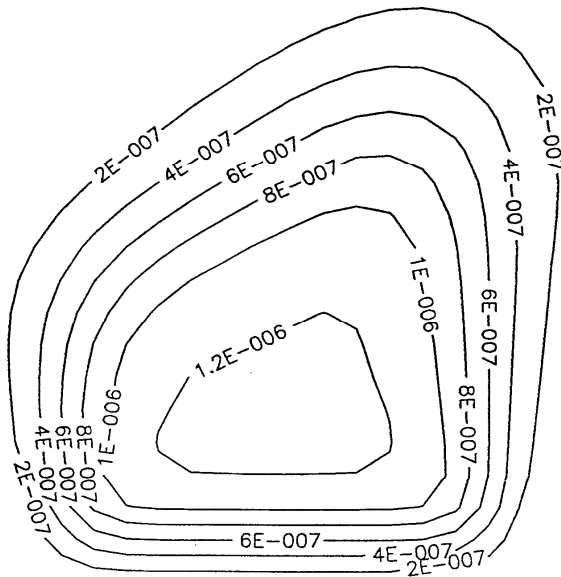
Figure 4. Receptor-time averaged concentrations resulting from numerical integration of the evolution of the slug depicted in Figure 3 from its initial (left) to its final (right) "snapshot" states. [From Scire et al., 1990b]

The variable ξ in Eq.(16) can also be written as the function:

$$\xi \equiv \frac{d_{a2} - u \cdot \Delta t_S \cdot (t / \Delta t_S)}{\sqrt{2}\sigma_y} \tag{18}$$

of the dimensionless time variable $(t/\Delta t_S)$, where $0 \leq t/\Delta t_S \leq 1$, such that $\xi = \xi_b + (\xi_e - \xi_b) \cdot (t/\Delta t_S)$, with $\xi_b \equiv \dfrac{d_{a2}}{\sqrt{2}\sigma_y}$ and $\xi_e \equiv \dfrac{d_{a2} - u \cdot \Delta t_S}{\sqrt{2}\sigma_y}$, as defined following Eq.(16b), so that the causality function of Eq.(14c) can be written:

$$F = \frac{1}{2} \cdot \{erf(\phi_2) - erf(\xi)\} \tag{19}$$

Thus, the time averaging process yields:

$$\overline{C}(x,y,z) = \frac{1}{U} \cdot P'(Y,\sigma_y) \cdot P(Z,\sigma_z) \cdot \{Q_b \cdot \overline{F}_0 + (Q_e - Q_b) \cdot \overline{F}_1\} \tag{20}$$

where $\overline{F}_0$ is $\overline{F}$ from Eq.(16b) and

$$\overline{F}_1 = \int_0^{\Delta t_S} \frac{dt}{\Delta t_S} \cdot \left(\frac{t}{\Delta t_S}\right) \cdot F(t) = \frac{1}{\Delta\xi} \int_{\xi_b}^{\xi_e} d\xi \cdot \left(\frac{\xi - \xi_b}{\Delta\xi}\right) \cdot F(\xi) \tag{21}$$

with $\Delta\xi \equiv \xi_e - \xi_b = \dfrac{-u \cdot \Delta t_S}{\sqrt{2}\sigma_y}$. Substituting in Eq.(19) into Eq.(21) then yields:

$$\overline{F}_1 = \frac{1}{4} \cdot erf(\phi_2) - \frac{1/2}{(\Delta\xi)^2} \left\{ \int_\xi^{d\xi_e} d\xi \cdot \xi \cdot erf(\xi) - \xi_b \cdot \int_\xi^{\xi_e} d\xi \cdot erf(\xi) \right\} \tag{22}$$

where the integral, $\int dx \cdot erf(x) = x \cdot erf(x) + \dfrac{1}{\sqrt{\pi}} \cdot \exp(-x^2)$, has already been used to obtain Eq.(16b) and where the integral, $\int dx \cdot x \cdot erf(x) = \dfrac{1}{2} \cdot x^2 \cdot erf(x) + \dfrac{1}{2} \cdot \dfrac{x}{\sqrt{\pi}} \cdot \exp(-x^2) - \dfrac{1}{4} \cdot erf(x)$, is a special case of the more general expression developed by Geller and Ng (1971) in terms of the generalized hypergeometric function $_2F_2$.

Generalizing the problem of dealing with older slugs is straightforward if one chooses a numerical integration (i.e., time-average) of Eq.(14). The time dependent expression $Q(t)$ given by Eq.(17) simply replaces Q and the numerical integration proceeds.

However, this numerical integration process has itself received special attention because it greatly influences the computing time needs of the slug model. First, all receptors lying outside of the slug's $\pm$ 3 Φ_y envelope during the entire averaging time interval are eliminated from consideration. Second, for those receptors remaining, integration time limits are computed such that sampling is not performed when the receptor is outside of the $\pm$ 3 Φ_y envelope.

Invocation of the "frozen Φ" methodology (i.e., Φ_y and Φ_z are fixed at receptor-specific values throughout the averaging time period) creates another class of situations which can be integrated analytically; however, the most general case involves indefinite integrals of the form:

$$\int dt \cdot \exp(-\beta^2 \cdot t^2) \cdot erf(a + b \cdot t) \tag{23}$$

which defy solution except in a few simple cases (e.g., a = 0 and b = $\exists$). In fact, integrability has proven not to be the sole criteria in these slug sampling problems. For example, the preceding work on linear time variation of loss (or production) mechanisms can also be evaluated for the more realistic exponential process; however, the analytic forms are found to be very volatile on a computer because subtraction of large numbers to obtain small numbers is required.

One tractable case involves the quite physical scenario of a slug passing rapidly over a receptor and with slug endpoints sufficiently far away that the along-slug causality factor, $F(t)$, is time independent. In this case, the causality factor also becomes fixed and can be taken outside the integral and approximated as:

$$\overline{F} = \frac{1}{2} \cdot (F_b + F_e) \tag{24}$$

which is just the average of values at the beginning and end of the time step. This approximation is, however, made only if F_b and F_e are within a specified small fractional tolerance of each other. A similar procedure enables one to move the vertical coupling factor, $P(Z,\sigma_z)$, outside the integral and replace it with the mean value, $\overline{P}$, provided that the initial and final values are within a small tolerance window (e.g., a few percent). Finally, the variability of the lateral coupling term of Eq.(14b) to temporal variation of the crosswind distance, $d_c(t)$, is checked and the integrals:

$$I_m = \int\limits_0^{\Delta t_S} \frac{dt}{\Delta t_S} \cdot \left(\frac{t}{\Delta t_S}\right)^m \cdot P'[\eta(t), \sigma_y] \tag{25}$$

with $P'(\eta(t), \sigma_y) \equiv \dfrac{1}{\sqrt{2\pi}\sigma_y} \cdot \exp\left[-\eta^2(t)\right]$ and $\eta(t) \equiv \dfrac{1}{\sqrt{2}} \cdot \dfrac{d_c(t)}{\sigma_y} \cdot \dfrac{u}{U}$ evaluated for

m = 0 and 1. These integrals can be solved to yield:

$$I_0 = \frac{\sqrt{\pi}}{2} \cdot \frac{[erf(\eta_e) - erf(\eta_b)]}{(\eta_e - \eta_b)} \quad \text{and} \quad I_1 = \frac{1}{2} \cdot \frac{[\exp(-\eta_e^2) - \exp(-\eta_b^2)]}{(\eta_e - \eta_b)^2} - \frac{\eta_b \cdot I_0}{(\eta_e - \eta_b)} \quad (26)$$

so that the final, time-averaged concentrations can be written as:

$$\overline{C}(x,y,z) = \frac{\overline{F} \cdot \overline{P}(Z,\sigma_z)}{\sqrt{2\pi} \cdot \sigma_y \cdot U} \cdot \{Q_b \cdot I_0 + (Q_e - Q_b) \cdot I_1\} \quad (27)$$

as an alternative to numerical integration for some older slugs.

Vertically integrated counterparts to Eq.(20) and Eq.(27) are also required in CALPUFF for evaluation of wet removal and wet fluxes at a ground level receptor; however, given the normalization properties of the Gaussian, these are obtained by replacing $P(Z,\sigma_z)$ with 1.0 in Eq.(20) or $\overline{P}(Z,\sigma_z)$ with 1.0 in Eq.(27).

It should also be noted that decision logic in CALPUFF allows slugs in the near-field to transition to puffs in the far-field. This decision process is based primarily on the eccentricity of the overall slug shape; that is, axial slug length relative to the size of the horizontal dispersion coefficients at the slug end points. It should be noted in such conversion that one must have retained both the slug's effective emission rate, Q, as well as the original emission duration, t_E, for that slug, so that the slug mass of $Q \cdot t_E$ is available for puff computation purposes.

Both the original California ARB documentation (Scire et al., 1990b) and the more recent report on CALPUFF Version 5 (Scire et al., 2000) contain extensive documentation on the absolute and comparative accuracy and computation times of the various slug and puff formulations discussed herein.

In addition, several model evaluations using hour-average tracer concentrations have been performed (e.g., IWAQM, 1998; Strimaitis et al., 1998; Chang et al., 2003) and CALPUFF was found to be more reliable predictor of ambient concentrations than ISC3.

3   Puff Model Enhancements

The integrals discussed in the previous section lie at the heart of the CALPUFF model, but this model is now a comprehensive code exceeding 50K lines and includes a full range of phenomena that must now be explicitly considered. For example, CALPUFF has modules for many, near-source effects (e.g., plume rise, stack and building downwash, partial lid penetration), complex-terrain plume dynamics, mass depletion (e.g., dry and wet deposition) and transformation mechanisms, and specialized meteorological conditions (e.g., fog). The CALPUFF modeling system also contains a graphical interface for setting up and managing runs; preprocessor programs for emissions, meteorology, land-use,

terrain and other input files; and postprocessor programs for various longer-term concentration averages and visibility. An exposition of most of these features is beyond the scope of this chapter; however, in the following subsections, we consider some phenomena that are fundamental to the puff model itself.

3.1   Dispersion Coefficients for Puff Modeling

Short duration pollutant releases and human exposures can have important consequences: toxic gas releases and odor impacts being among the clearer examples. Historically, puff models have been developed with an emphasis on predicting one-hour (and longer) average concentrations on meso- through regional-scale domains. Hence, the model's basic time step for taking in new meterology (e.g., a specific wind speed and direction at each source) was one hour or longer, and the dispersion coefficients were tailored to reflect all dispersive mechanisms that contribute during a corresponding averaging time interval. That is, the dispersion rate of individual puffs is effectively convoluted with the lower frequency meandering of wind direction to yield overall dispersion coefficients that in-turn yield reasonable, hourly or multi-hour average concentrations. More specifically, in the case of CALPUFF, regulatory dispersion coefficient schemes were chosen so predicted concentrations would exactly match the results of the Gaussian plume ISC3 model (i.e., if CALPUFF is run using steady-state emissions and meteorology conditions for a sufficiently long time to avoid "transients" associated with initiation of emissions or the "causality" lag associated with source to receptor transport).

One way to account for shorter, time-average concentrations in CALPUFF is to allow input of peak-to-mean concentration ratio factors into CALPUFF's post-processor program (i.e., CALPOST). This feature improves the utility of CALPUFF in applications involving odor and short-term toxic exposure problems.

To more realistically simulate shorter averaging time periods when suitable meteorological data are available, the most recent version of CALPUFF (i.e., Version 6) pemits updates of meteorological fields as often as once per minute. Optimal use of this rapid-update feature requires that the dispersion coefficients be appropriately matched to the meteorological field update interval.

Traditionally, such shorter averaging-time quantities have been estimated from longer-time-averaged measured data via the averaging-time power-law scaling:

$$\sigma(\tau_1) \approx (\tau_1/\tau_2)^p \cdot \sigma(\tau_2) \tag{28a}$$

where τ_1 and τ_2 are the two relevant averaging times, and p is the appropriate power-law exponent. For averaging times shorter than one hour, a value of $p = 0.2$ for τ in the range of 3 - 60 minutes has been suggested by Gifford (1975) for σ_y; whereas, smaller exponents over a more limited range of averaging times

(e.g., 3 - 20 min.) are considered for σ_z (Pasquill, 1976). Discussion continues over the importance (Hanna et al., 2003) and appropriateness (Venkatram, 2002) of making such power-law corrections for averaging time. Currently, CALPUFF permits averaging time corrections, of the type expressed by Eq.(28a), to be made only for the Pasquill-Gifford σ_y dispersion curves. The other parameterized dispersion curves available for use in CALPUFF cannot be so scaled, as appropriate guidance does not appear in the literature.

Another dispersion coefficient alternative for short averaging times that is presently offered within CALPUFF is the ability to compute dispersion coefficients based on locally measured values of turbulence (i.e., σ_v and σ_w) and the formulae:

$$\sigma_y = \sigma_v \cdot t \cdot f_y(t/\tau_y) \qquad \text{and} \qquad \sigma_z = \sigma_w \cdot t \cdot f_z(t/\tau_z) \tag{28b}$$

where $f_y(t/\tau_y) = 1.0 / [1.0 + 0.9 \cdot (t/\tau_y)^{1/2}]$ and $f_z(t/\tau_y) = 1.0 / [1.0 + a \cdot (t/\tau_y)^p]$, with $(a, p) = (0.9, 0.5)$ for unstable conditions and $(0.945, 0.806)$ for stable conditions. This Eq.(28b) approach to dispersion uses Irwin's (1983) recommended implementation of Draxler's (1976) forms for the f_y and f_z functions, and currently incorporates a fixed value for τ_y of 1000s and fixed values for τ_z of 500s and 100s for unstable and stable conditions, respectively.

Unfortunately, the validity of Eq.(28b), including the appropriate forms for f_y and f_z and their accompanying coefficients and time scales, has not yet been extensively evaluated for short averaging times.

The most elegant approach to modeling short averaging times would be to build in a model option to choose true "puff sigmas"; however, appropriate formulations are not widely available over a significant range of transport times and dispersion conditions. A series of true puff tracer release experiments (e.g., BOREX89, BORRIS94, GUARDO, MADONA, FLADIS, COFIN) were recently performed, and an analysis by Mikkelsen et al. (2002) of several such experiments combined suggests a linear time-dependent puff growth law of:

$$\sigma_{puff}(t) \approx 0.73 \cdot U_* \cdot t \tag{29}$$

where U_*(m/s) is the surface friction velocity and t(s) is puff travel time. Equation (29) was found to be appropriate for near-surface releases and has been confirmed only for $\sigma_{puff}(t) \leq 25$m. Of course, such early-phase puff growth gives way to a period of accelerated $t^{3/2}$ growth (Richardson, 1926; Batchelor, 1950), which has been observed (Gifford, 1977), and concludes with Taylor's (1921) $t^{1/2}$ growth (i.e., which may or may not ever be observed due to the eventual dominance of wind shear induced growth).

It is interesting to note that the coefficient of 0.73 is about half of that used in typical, turbulence-based, dispersion coefficients [e.g., $\sigma_y = 1.6 \cdot U_* \cdot t \cdot f(t/\tau_y)$ and

$\sigma_z = 1.3 \cdot U_* \cdot t \cdot f(t/\tau_z)$] that may be computed within CALPUFF (i.e., when the turbulence-based dispersion option is chosen and the turbulence is computed from surface-layer formulae). These larger coefficients of $U_* \cdot t$ result from the fact that these larger dispersion coefficients include a significant wind-meander component along with the true puff dispersion.

Clearly, if puff sigmas are employed, then some explicit formulation of wind direction meander, such as that of Oettl et al. (2005), also ought to be available for the computation of the concentration cumulative frequency distribution and/or longer time averages.

3.2   Wind Shear Effects on Puffs

While puff models are often driven by a wind field model that allows for spatially and varying wind fields, the entire puff is usually just transported by the wind at the center of the puff, such that wind gradients or shears are ignored. In some cases, the accumulated wind shear is tracked and, when large enough, leads to a splitting of the puff into two or more puffs. However, the successful incorporation of shear into plume models [i.e., Walcek (2004) as discussed in Chap. 7B], leads one to ask if this could also be done for puff models.

The reason the puff model formulations generally ignore explicit shear is that they stem from the solution of the diffusion equation with an assumed diagonal diffusivity matrix. That is, they begin with the diagonal diffusivity matrix, $\mathbf{K}_d$, rather that the full diffusivity matrix, $\mathbf{K}$, where both are given as:

$$\mathbf{K}_d = \begin{bmatrix} K_{xx} & 0 & 0 \\ 0 & K_{yy} & 0 \\ 0 & 0 & K_{zz} \end{bmatrix} \quad \text{and} \quad \mathbf{K} = \begin{bmatrix} K_{xx} & K_{xy} & K_{xz} \\ K_{yx} & K_{yy} & K_{yz} \\ K_{zx} & K_{zy} & K_{zz} \end{bmatrix} \tag{30}$$

Now the $\mathbf{K}_d$ form of the diffusivity matrix leads to the well-known puff solution:

$$C(x,y,z,t) = \frac{m}{(2 \cdot \pi)^{3/2} \cdot \sqrt{8 \cdot K_{xx} \cdot K_{yy} \cdot K_{yy} \cdot t^3}} \cdot \exp\left[\frac{-1}{4 \cdot t} \cdot \left\{ \frac{(x-x_c)^2}{K_{xx}} + \frac{(y-y_c)^2}{K_{yy}} + \frac{(z-z_c)^2}{K_{zz}} \right\}\right] \tag{31}$$

where m is the mass within the puff. Replacing the terms $2 \cdot K \cdot t$ with their equivalent σ^2 then leads back to the Eq.(3) form introduced earlier.

Unfortunately, Eq.(31) does not allow for the introduction of puff-distorting wind shear terms; however, expansion of the basic advection-diffusion equation [i.e., Eq.(2)] in terms of Taylor series for the winds and concentrations shows (e.g., Yamartino, 2000) that one can include the effects of wind shears either through

purely advective terms or via diffusive terms involving the off-diagonal terms of the full K matrix.

The less well-known solution to the full diffusivity matrix form (Anderson, 1984; Wegener and Schroeter, 1995) can be written for an arbitrary number of dimensions, n, as:

$$C(x,y,z,t) = \frac{m}{(2 \cdot \pi)^{n/2} \cdot |D|^{1/2} \cdot (2 \cdot t)^{n/2}} \cdot \exp\left[-\frac{1}{4 \cdot t} \mathbf{X}^T \mathbf{K}^{-1} \mathbf{X}\right] \qquad (32a)$$

where for n = 3, $\mathbf{X} = \begin{bmatrix} x - x_c \\ y - y_c \\ z - z_c \end{bmatrix}$ is a column vector, $\mathbf{K}^{-1} = \begin{bmatrix} K_{xx} & K_{xy} & K_{xz} \\ K_{yx} & K_{yy} & K_{yz} \\ K_{zx} & K_{zy} & K_{zz} \end{bmatrix}^{-1}$ is the

inverse of the 3D diffusivity matrix $\mathbf{K}$, $\mathbf{X}^T = [x - x_c, y - y_c, z - z_c]$ is the transpose row vector, with (x_c, y_c, z_c) being the center coordinates of the puff, and $|D|$ is the determinant of matrix $\mathbf{K}$. It is also useful to know that Eq.(32a) can alternatively be written in terms of the dispersion sigmas as:

$$C(x,y,z,t) = \frac{q}{(2 \cdot \pi)^{n/2} \cdot |D|^{1/2}} \cdot \exp\left[-\frac{1}{2} \mathbf{X}^T (\mathbf{\sigma^2})^{-1} \mathbf{X}\right] \qquad (32b)$$

where $(\mathbf{\sigma^2})^{-1} = \begin{bmatrix} \sigma_x^2 & \sigma_{xy}^2 & \sigma_{xz}^2 \\ \sigma_{yx}^2 & \sigma_y^2 & \sigma_{yz}^2 \\ \sigma_{zx}^2 & \sigma_{zy}^2 & \sigma_z^2 \end{bmatrix}^{-1}$ and $|D|$ is the determinant of matrix σ^2.

Expanding the n = 3 solution for the inverse K^{-1} yields the rather messy result:

$$\mathbf{K}^{-1} = \frac{1}{|D|} \begin{bmatrix} +(K_{yy} \cdot K_{zz} - K_{yz} \cdot K_{zy}) & -(K_{xy} \cdot K_{zz} - K_{xz} \cdot K_{zy}) & +(K_{xy} \cdot K_{yz} - K_{xz} \cdot K_{yy}) \\ -(K_{yx} \cdot K_{zz} - K_{yz} \cdot K_{zx}) & +(K_{xx} \cdot K_{zz} - K_{xz} \cdot K_{zx}) & -(K_{xx} \cdot K_{yz} - K_{xz} \cdot K_{yx}) \\ +(K_{yx} \cdot K_{zy} - K_{yy} \cdot K_{zx}) & -(K_{xx} \cdot K_{zy} - K_{xy} \cdot K_{zx}) & +(K_{xx} \cdot K_{yy} - K_{xy} \cdot K_{yx}) \end{bmatrix} \quad (33a)$$

where

$$|D| = [K_{xx} \cdot (K_{yy} \cdot K_{zz} - K_{yz} \cdot K_{zy}) - K_{yx} \cdot (K_{xy} \cdot K_{zz} - K_{xz} \cdot K_{zy}) + K_{zx} \cdot (K_{xy} \cdot K_{yz} - K_{xz} \cdot K_{yy})] \quad (33b)$$

One notes that the 2D, y-z plume solution appears much simpler as:

$$\mathbf{K} = \begin{bmatrix} K_{yy} & K_{yz} \\ K_{zy} & K_{zz} \end{bmatrix} \quad \text{and} \quad \mathbf{K}^{-1} = \frac{1}{|D|}\begin{bmatrix} +K_{zz} & -K_{yz} \\ -K_{zy} & +K_{yy} \end{bmatrix} \tag{34a}$$

with determinant,

$$|D| = (K_{yy} \cdot K_{zz} - K_{yz} \cdot K_{zy}) \tag{34b}$$

Comparison with the plume solution of Walcek [see Chapter 7B, Eq.(45)] suggests that:

$$(1 - \frac{K_{yz} \cdot K_{zy}}{K_{yy} \cdot K_{zz}}) = 1 + s^2/12 \quad \text{where } s \equiv \frac{\partial v}{\partial z}\cdot\frac{x}{u}\sqrt{\frac{K_{zz}}{K_{yy}}}. \tag{34c}$$

If one further assumes that $K_{zy} = -K_{yz}$, as is necessary to achieve the sign flip between the left and right sides of Eq.(34c), then one concludes that Walcek's plume solution requires[2]:

$$\frac{K_{yz}}{\sqrt{K_{yy}\cdot K_{zz}}} = \frac{1}{\sqrt{12}}\cdot\frac{\partial v}{\partial z}\cdot\sqrt{\frac{K_{zz}}{K_{yy}}}\cdot\frac{x}{u} = \frac{1}{\sqrt{12}}\cdot\frac{\partial v}{\partial z}\cdot\sqrt{\frac{K_{zz}}{K_{yy}}}\cdot t. \tag{35}$$

This is fine, except that a K ratio proportional to travel time, t, shows that the needed solution for a constant crosswind velocity shear, $(\partial v/\partial z)$, does not simply involve the purely, space-time invariant K values usually assumed for the Eq.(32) solution of the time-dependent diffusion equation in n dimensions.

Nevertheless, for the puff, we consider the case of the two most important velocity shears: $u_z \equiv (\partial u/\partial z)$ and $v_z \equiv (\partial v/\partial z)$. This means that the determinant will now appear as:

$$|D| = [K_{xx}\cdot(K_{yy}\cdot K_{zz} - K_{zy}\cdot K_{yz}) - K_{xz}\cdot K_{zx}\cdot K_{yy})] = [K_{xx}\cdot K_{yy}\cdot K_{zz}\cdot(1 - \frac{K_{zy}\cdot K_{yz}}{K_{yy}\cdot K_{zz}} - \frac{K_{xz}\cdot K_{zx}}{K_{xx}\cdot K_{zz}})$$

  or   (36a)

$$|D| = K_{xx}\cdot K_{yy}\cdot K_{zz}\cdot\left[1 + \frac{(s_u^2 + s_v^2)}{12}\right] \quad \text{and} \quad |D| = \sigma_x^2\cdot\sigma_y^2\cdot\sigma_z^2\cdot\left[1 + \frac{(s_u^2 + s_v^2)}{12}\right]$$

for the K and σ^2 representations, respectively,

---

[2] Symmetry suggests a full K_{yz} of: $K_{yz} = \frac{1}{\sqrt{12}}\cdot\frac{\partial v}{\partial z}\cdot\frac{x}{u}\cdot K_{zz} - \frac{1}{\sqrt{12}}\cdot\frac{\partial w}{\partial y}\cdot\frac{x}{u}\cdot K_{yy}$

where the added substitutions:

$$\frac{K_{xz}}{K_{zz}} = \frac{1}{\sqrt{12}} \cdot \frac{\partial u}{\partial z} \cdot \frac{x}{u} = \frac{1}{\sqrt{12}} \cdot \frac{\partial u}{\partial z} \cdot t \ , \tag{36b}$$

$$s_v \equiv \frac{\partial v}{\partial z} \cdot t \cdot \sqrt{\frac{K_{zz}}{K_{yy}}} = \frac{\partial v}{\partial z} \cdot t \cdot \frac{\sigma_z}{\sigma_y} \ , \ \text{and} \ \ s_u \equiv \frac{\partial u}{\partial z} \cdot t \cdot \sqrt{\frac{K_{zz}}{K_{xx}}} = \frac{\partial u}{\partial z} \cdot t \cdot \frac{\sigma_z}{\sigma_x} \ \ \text{are used.} \tag{36c}$$

Thus far, the 3D K matrix approach is useful, as it has yielded the correct form of $|D|$; however, continuing further with the K matrix strategy requires one to specify the K_{xy} term, and this is not obvious nor can it be neglected. Instead, we step back to the Walcek solution [Chapter 7B, Eq.(45)], add in the x-component ingredient of the puff formulation, and temporarily ignore uniform advection (i.e., as the principle of translational invariance will always permit us to re-inject uniform advection). Without uniform advection, there is no preferred orientation for the x-y axes, except for the directionality dictated by shear. Thus, imagine a coordinate system where the effective total shear is aligned along the y' axis. In this case, one might guess the equivalent puff solution to be:

$$C(x,y,z) = \frac{m}{(2\pi)^{3/2} \cdot \sigma_x \cdot \sigma_y \cdot \sigma_z \cdot f} \cdot \exp\left[-\frac{1}{2}\left\{\frac{x'^2}{\sigma_h^2} + \frac{y'^2}{f^2 \cdot \sigma_h^2} + \frac{(z-z_S)^2 \cdot (1+s^2/3)}{f^2 \cdot \sigma_z^2} - \frac{(z-z_S) \cdot y' \cdot s}{f^2 \cdot \sigma_h \cdot \sigma_z}\right\}\right] \tag{37a}$$

where σ_h is the lateral dispersion coefficient,

and as before,

$$f^2 \equiv 1 + s^2/12 \ \ \text{and} \ \ s^2 \equiv s_u^2 + s_v^2. \tag{37b}$$

Given that Walcek's 2D solution conserves mass, one can be quite sure that Eq.(37a) will at least conserve mass in 3D. Now, one simply rotates back from the (x', y') axes to the usual (x, y) frame via substitutions:

$$y' = y \cdot cos(\theta) + x \cdot sin(\theta) \ \text{and} \ x' = x \cdot cos(\theta) - y \cdot sin(\theta) \tag{37c}$$

where

$$sin(\theta) = s_u / s \ \text{and} \ cos(\theta) = s_v / s \tag{37d}$$

After expanding the substitutions, collecting terms, and re-inserting uniform advection, one recovers the full puff solution of:

$$C(x,y,z,t)=\frac{m}{(2\cdot\pi)^{3/2}\cdot\sigma_x\cdot\sigma_y\cdot\sigma_z\cdot f}\cdot\exp\left[\frac{-1}{2\cdot f^2}\left\{\begin{array}{c}\dfrac{f_v^2\cdot x''^2}{\sigma_x^2}+\dfrac{f_u^2\cdot y''^2}{\sigma_y^2}+\dfrac{z''^2\cdot(1+s^2/3)}{\sigma_z^2}\\[2ex]-\dfrac{x''\cdot y''\cdot s_u\cdot s_v}{6\cdot\sigma_x\cdot\sigma_y}-\dfrac{x''\cdot z''\cdot s_u}{\sigma_x\cdot\sigma_z}-\dfrac{y''\cdot z''\cdot s_v}{\sigma_y\cdot\sigma_z}\end{array}\right\}\right] \quad\text{(38a)}$$

where

$$f_u^2\equiv 1+s_u^2/12\,,\qquad\qquad\qquad f_v^2\equiv 1+s_v^2/12\,, \quad\text{(38b)}$$

$$x''\equiv x-\{x_0+[u_0+\tfrac{1}{2}\cdot(\partial u/\partial z)\cdot w_0\cdot t]\cdot t\}\,,\quad y''\equiv y-\{y_0+[v_0+\tfrac{1}{2}\cdot(\partial v/\partial z)\cdot w_0\cdot t]\cdot t\}\,,$$

and

$$z''\equiv z-(z_0+w_0\cdot t) \quad\text{(38c)}$$

with $(x_0,\ y_0,\ z_0)$ and $(u_0,\ v_0,\ w_0)$ being the coordinates and winds at time $t = 0$. These initial values are typically the coordinates and winds at the source. Note also that any vertical velocity component, w_0, is assumed to be constant over the time period t.

Verification that Eq.(38) is indeed a solution of the diffusion equation requires that one switch back to the K representation by substituting $\sigma^2 = 2\cdot K\cdot t$ everywhere (and with appropriate subscripts). The number of terms involving time, t, is quite intimidating, such that evaluation of whether Eq.(38) is a solution of the diffusion equation,

$$\frac{\partial C}{\partial t}+u\cdot\frac{\partial C}{\partial x}+v\cdot\frac{\partial C}{\partial y}+w\cdot\frac{\partial C}{\partial z}-K_{xx}\cdot\frac{\partial^2 C}{\partial x^2}-K_{yy}\cdot\frac{\partial^2 C}{\partial y^2}-K_z\cdot\frac{\partial^2 C}{\partial z^2}=0 \quad\text{(39a)}$$

is best accomplished using a computer algebra program, such as Maple (i.e., a software package sold commercially by Waterloo Maple, Inc.) or Mathematica (i.e., a software package sold commercially by Wolfram Research, Inc.). This has been done and Eq.(38a) is indeed an exact solution of Eq.(39a).

One might immediately question why the off-diagonal diffusivity terms don't appear in Eq.(39). The answer is that the off-diagonal terms, such as:

$$K_{xz}\cdot\frac{\partial^2 C}{\partial x\cdot\partial z}+K_{zx}\cdot\frac{\partial^2 C}{\partial z\cdot\partial x}=0 \quad\text{(39b)}$$

all vanish for pure wind-shear related diffusivities, as $K_{xz} = -K_{zx}$ are antisymmetric in their subscript indices, and the equality of the partial second derivatives, such as:

$$\frac{\partial^2 C}{\partial x \cdot \partial z} = \frac{\partial^2 C}{\partial z \cdot \partial x} \tag{39c}$$

is almost always guaranteed for C given by analytic functions. Note that if the off-diagonal diffusivity terms contained true diffusion components, these portions of the off-diagonal K elements would be symmetric, and addition rather than cancellation would occur.

The solution provided by Eq.(38) is quite interesting and worthy of further analysis. First, one notes that the shear-altered, puff-center concentration, C_c', (i.e., at $x'' = y'' = z'' = 0$) is reduced by the factor $1/f$ (i.e., $C_c' = C_c / f$). Thus, even though shearing per se is distortional and not diffusive, the combination of shear in concert with diffusion leads to the reduced puff-center concentration.

It is also interesting to note what has happened to the standard deviations of the sheared distribution (i.e., σ_x', σ_y', σ_z') relative to the original, unsheared moments (i.e., σ_x, σ_y, σ_z). Actually, there can be several different interpretations of what is meant by the second moment. For example, if one were to evaluate the effective σ_x' in Eq.(38a) through the puff center, as defined by the line $y'' = z'' = 0$, simple inspection of Eq.(38a) would show an increased standard deviation of:

$$\sigma_x' = \sigma_x \cdot f / f_v \xrightarrow[s_v \to 0]{} \sigma_x \cdot (1 + s_u^2 / 12)^{1/2} \tag{40a}$$

in agreement with the result presented by F. B. Smith (1965), and in agreement with along-wind diffusion parameterizations employed by Wilson (1981) and Hanna and Franzese (2000). Similarly the effective σ_y' through the puff center, as defined by the line $x'' = z'' = 0$, would yield the increased value of:

$$\sigma_y' = \sigma_y \cdot f / f_u \xrightarrow[s_u \to 0]{} \sigma_y \cdot (1 + s_v^2 / 12)^{1/2} . \tag{40b}$$

However, the effective σ_z' through the puff center, defined by the line $x'' = y'' = 0$, would surprizingly yield the reduced value of:

$$\sigma_z' = \sigma_z \cdot \frac{(1 + s^2 / 12)^{1/2}}{(1 + s^2 / 3)^{1/2}} \tag{40c}$$

How could the plume shrink in this vertical dimension as there is no shear stretching or enhanced diffusivity in this dimension? The truth is that the plume has not physically shrunk in the z-dimension, but the fact that the diffused ellipsoid has been rotated away from its original principal axes means that the line specified by $x'' = y'' = 0$ is no longer along a major/minor axes, but rather cuts obliquely through the ellipsoid.

However, if one first integrates Eq.(38a) over the entire x''-y'' plane and then re-evaluates the vertical second moment, one would find that this projection of the entire distribution onto the z''-axis was indeed associated with an unchanged standard deviation of:

$$\sigma'_z = \sigma_z \, . \tag{41a}$$

Performing similar analyses on the integrated projections onto the x'' and y'' axes, respectively, yields standard deviations of :

$$\sigma_x' = \sigma_x \cdot (1 + s_u^2 / 3)^{\frac{1}{2}} \quad \text{and} \quad \sigma_y' = \sigma_y \cdot (1 + s_v^2 / 3)^{\frac{1}{2}} \, . \tag{41b}$$

As these standard deviations represent a full projection of the entire puff distribution rather than a slice through a single point (i.e., the puff center), it is not surprising that each of these three standard deviations are larger than the corresponding standard deviation presented in Eq.(40). Thus, the moments one obtains are sensitive to the constraints placed upon the computational procedure, and more specifically, sensitive to the specific projection that is being considered. As a final example of this, consider Eq.(38a) on the plane $z'' = 0$, then integrate over y'', and finally evaluate the variance in x''. This will lead to the exact results:

$$\sigma'_x = \sigma_x \cdot (1 + s_u^2 / 12)^{1/2} \qquad \text{and} \qquad \sigma'_y = \sigma_y \cdot (1 + s_v^2 / 12)^{1/2} \tag{42}$$

where the σ'_y result arises from the corresponding consideration of $z'' = 0$, integration over x$''$, and finally evaluation of the variance in y$''$.

The solution of the sheared puff problem may also be approached using Fourier Transforms (FT). Recently, R. B. Smith (2005) has done a thorough analysis of the sheared puff solution in FT space, and obtains a general solution of the FT of the concentration distribution in terms of the spatial FT of the source distribution. Inversion of this solution via rapid inverse transform algorithms (i.e., Fast Fourier Transform or FFT software) provides an efficient means for evaluating concentration distributions as well as obtaining interesting results on the distribution of tracer ages within a sheared puff. Smith also finds that the FT approach yields first and second concentration distribution moments in agreement with the earlier work of Saffman (1962). While there is agreement between their estimate of the vertical standard deviation σ'_z and the unchanged standard deviation of Eq.(41a), their estimates for the altered σ'_x and σ'_y are considerably smaller [i.e., $(7/30 - \pi/16)/2 \approx 0.018491$ versus the $1/12 \approx 0.083333$] than those presented in Eq.(40b). This factor of 4.5 difference in the σ^2 (i.e., a factor of 2.12 in the σ) was also derived by F. B. Smith(1965) (see also Pasquill and Smith, 1983) and can be understood by recognizing that Eq.(38a) is the solution for the unbounded puff, such that shear can be viewed as symmetric about the puff's center; however, Saffman (1962) and R. B. Smith (2005) treat the case of the semi-bounded puff (i.e., a ground level release described by the unbounded puff solution above ground plus its reflection term below ground). To compute the

reflection term equivalent to Eq.(38a), one must recognize that the shears, s_u and s_v of Eq.(36c), <u>flip sign</u> in the ground reflection terms. Thus, rather than a puff sheared symmetrically about its center, one has a half-puff shape sheared asymmetrically and subjected to net overall transport. Intuitively, one might imagine that the shear sign flip in the reflection term would yield a factor-of-two smaller, shear-induced sigma (rather than the factor of 2.12 mentioned above); however, the asymmetry of this sheared, "half-puff" shape accounts for the deviation from a strict factor-of-two. Note that when evaluating the standard deviation of this half-puff shape, one must account for the net advective displacement via the computational rule: variance equals mean-square minus the mean squared, or:

$$\sigma_x^2 = [<C \cdot x^2> - <C \cdot x>^2]/<C> \tag{43}$$

where $<>$ denotes integration over the domain and variable (i.e., dx) of interest.

Finally, returning briefly to Eq.(38), one notes that the formulation includes mean velocity components, u_0, v_0, and w_0, and that the coordinates x, y, z, represent an arbitrary orthogonal system and do not reflect a "preferred" frame, such as used in plume modeling, where x is meant to imply the along-wind direction. Thus, Eq.(38) can easily be adapted to a multi-time-step model where u_0, v_0, and w_0 can change with each new time step. This adaption is accomplished through the use of "initial sigmas" and various pseudo-times, t_0, such that the $t = 0$ point at the beginning of the next time step is associated with the $t = \Delta t$ state of the Eq.(38a) distribution at the end of the previous time step. Thus, Eq.(38a) can be advanced over many time steps with varying meteorology without needing to consider computationally-expensive measures such as puff-splitting. Of course, at some point, the puff may become so sheared that its top and bottom are in different meteorological grid cells (i.e., possibly having totally different flow and turbulence characteristics), and, in such cases, it will be necessary to split the puff. In this case, it may be most appropriate to break the single ellipsoid, characterizing the distribution, into two (or more) ellipsoids.

3.3   Modeling of Higher Concentration Moments

As far back as the mid-1980s, Sykes and co-workers at Aeronautical Research Associates of Princeton (ARAP) were working on developing a series of higher-order closure based plume and puff models. One primary feature of this approach is that by expanding the concentration and velocity fields into mean and fluctuation components, Sykes *et al.* (1984) were able to develop a partial differential equation for the mean-square concentration, $<C^2>$. This implies that one is able to predict concentration variance, σ_c^2 (i.e., as $\sigma_c^2 = <C^2> - <C>^2$), along with the traditional mean concentration, $<C>$. The resulting puff model, SCIPUFF, employs second-order turbulence closure theory and solves the PDEs for mean and mean-squared concentration via numerical methods. The SCIPUFF model has undergone refinement and evaluation for more than a decade. Thus,

any attempt to fully and fairly describe SCIPUFF's equations and features and the technical aspects of yet other modeling approaches to predicting higher concentration moments and fluctuation measures would require an additional chapter and will not be attempted here. For those interested in SCIPUFF, the model and its extensive documentation are available online at:
http://www.titan.com/products-services/336/download_scipuff.html .

Acknowledgments

References

Abramowitz, M. and I.A. Stegun, 1972. Handbook of Mathematical Functions. NBS Applied Mathematics Series, Vol. 55, Tenth printing with corrections, Washington, D.C.   Now available online at: http://mintaka.sdsu.edu/faculty/wfw/ABRAMOWITZ-STEGUN/intro.htm   or   at: http://www.convertit.com/Go/ConvertIt/Reference/AMS55.ASP .

Anderson, T.W., 1984. An Introduction to Multivariate Statistical Analysis, 2nd Edition, John Wiley and Sons, New York, 675 pp.

Batchelor, G.K., 1950. The application of the similarity theory of turbulence of atmospheric diffusion. *Quart. J. Roy. Meteorol. Soc.*, **76**, 133-146.

Benkley, C.W. and A. Bass, 1979. Development of Mesoscale Air Quality Simulation Models. Volume 3. User's Guide to MESOPUFF (Mesoscale Puff) Model. EPA 600/7-79-XXX, Environmental Protection Agency, Research Triangle Park, NC, 124 pp.

Chang, J.C., P. Franzese and S.R. Hanna, 2000. Evaluation of CALPUFF, HPAC, and VLSTRACK with the Dipole Pride 26 Field Data. Proceedings, 11th Joint Conference on the Applications of Air Pollution Meteorology with the AWMA. American Meteorological Society, 45 Beacon St., Boston, MA 02108, pp. 340-346.

Chang, J.C., P. Franzese, K. Chayantrakom, and S.R. Hanna, 2003. Evaluations of CALPUFF, HPAC, and VLSTRACK with Two Mesoscale Field Datasets. *J. Appl. Meteor.*, **42**, 4, 453-466.

EPA, 1993. Interagency Workgroup on Air Quality Modeling (IWAQM) Phase I report: Interim recommendations for modeling long range transport and impacts on regional visibility. U.S. EPA, Research Triangle Park, NC.

Geller, M. and E. Ng, 1971. Tables of Integrals of the Error Functions - II: Additions and Corrections. *J. Res. National Bureau of Standards, Part B, Mathematical Sciences,* **75B**, 149-163.

Gifford, F.A., Jr., 1975.   Atmospheric Dispersion Models for Environmental Pollution Applications, in *Lectures on Air Pollution and Environmental Impact Analyses*, Boston, MA, Sept. 29-Oct. 3, pp. 35-38, American Meteorological Society, Boston, MA.

Gifford, F.A., Jr., 1976. Turbulent Diffusion - Typing schemes: A Review. *Nucl. Saf.*, **17**, 68-86.

Gifford, F.A., Jr., 1977. Tropospheric relative diffusion observations. *J. Appl. Meteorol.*, **16**, 311-313.

Hales, J.M., D.C. Powell and T.D. Fox, 1977: STRAM - An Air Pollution Model Incorporating Non-linear Chemistry, Variable Trajectories, and Plume Segment Diffusion. EPA 450/3-77-012. Environmental Protection Agency, Research Triangle Park, NC, 147 pp.

Hanna, S.R. and P. Franzese, 2000. Alongwind dispersion - A simple similarity formula compared with observations at 11 field sites and in one wind tunnel. *J. Appl. Met.*, **39**, 1700-1714.

Hanna, S.R., R. Britter, and P. Franzese, 2003. A baseline urban dispersion model evaluated with Salt Lake City and Los Angeles tracer data. *Atmos. Environ.*, **37**, 5069–5082.

Interagency Workgroup on Air Quality Modeling (IWAQM), 1998. Phase 2 Summary Report and Recommendations for Modeling Long Range Transport Impacts, EPA-454/R-98-019, U.S. Environmental Protection Agency.

Ludwig, F.L., L.S. Gasiorek and R.E. Ruff, 1977. Simplification of a Gaussian puff model for real-time minicomputer use. *Atmos. Environ.*, **11**, 431-436.

Mikkelsen, T., H. Jørgensen, M. Nielsen, and S. Ott, 2002. Similarity scaling of surface-released smoke plumes. *Boundary-Layer Meteorology*, **105**, 483-505.

Oettl, D., A. Goulart, G. Degrazia, and D. Anfossi, 2005. A new hypothesis on meandering atmospheric flows in low wind speed conditions, *Atmos. Environ.*, 39, 1739-1748.

Pasquill, F., 1976. Atmospheric Dispersion Parameters in Gaussian Plume Modeling. Part II. Possible Requirements for Change in the Turner Workbook Values. EPA-600/4-76-030b, 44 pp.

Pasquill, F. and F.B. Smith, 1984. Atmospheric Diffusion, 3rd Edition, Halsted Press Division of John Wiley and Sons, New York, 437 pp.

Prudnikov, A.P., Yu. A. Brychkov, and O.I Marichev, 1986. Integrals and Series, Volume 1, Elementary Functions. USSR Academy of Sciences, Moscow. Translated from the Russian by N.M. Queen, Gordon and Breach Science Publishers, New York.

Richardson, L.F., 1926. Atmospheric diffusion shown on a distance-neighbour graph. *Proc. Roy. Soc. London*, **A110**, 709-737.

Saffman, P.G., 1962. The Effect of Wind Shear on Horizontal Spread from an Instantaneous Ground Source, *Quart. J. Roy. Meteorol. Soc.*, **88**, 382–393.

Scire, J.S., E.M. Insley and R.J. Yamartino, 1990a. Model formulation and user's guide for the CALMET meteorological model. Prepared for the California Air Resources Board by Sigma Research Corporation, Concord, MA.

Scire, J.S., D.G. Strimaitis and R.J. Yamartino, 1990b. Model formulation and user's guide for the CALPUFF dispersion model. Prepared for the California Air Resources Board by Sigma Research Corporation, Concord, MA.

Scire, J.S., D.G. Strimaitis and R.J. Yamartino, 2000. User's guide for the CALPUFF dispersion model (Version 5). Earth Tech, Inc., Concord, MA.

Scire J.S., F.R. Robe, M.E. Fernau, and R.J. Yamartino, 1998. A User's Guide for the CALMET Meteorological Model (Version 5.0). Earth Tech, Inc., Concord, MA.

Scire, J.S., F.W. Lurmann, A. Bass and S.R. Hanna, 1984a. Development of the MESOPUFF II dispersion model. EPA-600/3-84-057, U.S. EPA, Research Triangle Park, NC.

Scire, J.S., F.W. Lurmann, A. Bass and S.R. Hanna, 1984b. User's guide to the MESOPUFF II model and related processor programs. EPA-600/8-84-013, U.S. Environmental Protection Agency, Research Triangle Park, NC.

Smith, F.B., 1965. The role of wind shear in horizontal diffusion of ambient particles. *Quart. J. Roy. Meteor. Soc.,* **91,** 318-329.

Smith, R.B., 2005. An analytical approach to shear dispersion and tracer age. *Boundary-Layer Meteorology*, **117**, 383–415.

Strimaitis, D.G., J.S. Scire and J.C. Chang, 1998. Evaluation of the CALPUFF Dispersion Model with two Power Plant Data Sets. Preprints 10th Joint Conference on the Applications of Air Pollution Meteorology, January 11-16, Phoenix, AZ.

Sykes, R.I., S.F. Parker, D.S. Henn, C.P. Cerasoli and L.P. Santos, 1998. PC-SCIPUFF Version 1.1PD.1 Technical Documentation. ARAP Report No. 718. Titan Corporation, Titan Research & Technology Division, ARAP Group, P.O. Box 2229, Princeton, NJ, 08543-2229. Available at: http://www.titan.com/products-services/336/download_scipuff.html .

Sykes, R.I. and D.S. Henn, 1995. Representation of velocity gradient effects in a Gaussian puff model. *J. Appl. Met.*, **34**, 2715-2723.

Sykes, R.I., W.S. Lewellen and S.F. Parker, 1984. A turbulent-transport model for concentration fluctuations and fluxes. *J. Fluid Mech.,* **139**, 193-218.

Taylor, G.I., 1921. Diffusion by continuous movements. *Proc. London Math. Soc.*, **20**, 196-211.

van Egmond, N.D. and H. Kesseboom, 1983. Mesoscale air pollution dispersion models - II. Lagrangian Puff model and comparison with Eulerian grid model. *Atmos. Environ.*, **17**, 267-274.

Venkatram, A., 2002. Accounting for averaging time in air pollution modeling. *Atmos. Environ.*, **36**, 2165–70.

Walcek, C.J., 2004. Accounting for wind shear in Gaussian dispersion models. American Meteorological Society 16th Symposium on Boundary Layers and Turbulence, Aug. 8-14. Portland, ME, Preprint 10.5.

Walcek, C.J., 2007. Accounting for wind shear in Gaussian dispersion models. *Atmos. Environ.*, In Press.

Wegener, R. and J. Schroeter, 1995. Correlational Kinetics, Part I: General Theory. *Physika A*, **219**, 159-188.

Wilson, D.J., 1981. Along-wind diffusion of source transients. *Atmos. Environ.*, **15**, 489-495.

Yamartino, R.J., 2000. Refinement of Horizontal Diffusion in Photochemical Grid Models. *Proc. 11 th Joint AMS/AWMA Conference on the Applications of Air Pollution Meteorology*, Long Beach, CA, January 9-14.

Zannetti, P., 1981. An improved puff algorithm for plume dispersion simulation. *J. Appl. Meteor.*, **20**, 1203-1211.